

RESEARCH ARTICLE | OCTOBER 06 2025

A highly efficient photodetector for squeezed light measurement in the gigahertz range

Dennis Wilken ; Jonas Junker ; Michèle Heurs 



Appl. Phys. Lett. 127, 144001 (2025)

<https://doi.org/10.1063/5.0290396>



Articles You May Be Interested In

Observation of amplitude squeezing in a constant-current-driven distributed feedback quantum dot laser with optical feedback

Quantum-enhanced super-sensitivity of Mach–Zehnder interferometer using squeezed Kerr state

7 dB quadrature squeezing at 860 nm with periodically poled K Ti O P O 4

Appl. Phys. Lett. (August 2006)



Applied Physics Letters

Special Topics Open
for Submissions

[Learn More](#)



A highly efficient photodetector for squeezed light measurement in the gigahertz range

Cite as: Appl. Phys. Lett. **127**, 144001 (2025); doi: 10.1063/5.0290396

Submitted: 11 July 2025 · Accepted: 11 September 2025 ·

Published Online: 6 October 2025



View Online



Export Citation



CrossMark

Dennis Wilken,^{1,a)}  Jonas Junker,^{1,2}  and Michèle Heurs^{1,3} 

AFFILIATIONS

¹Institute for Gravitational Physics, Leibniz University Hannover, 30167 Hannover, Germany

²Center for Macroscopic Quantum States (bigQ), Department of Physics, Technical University of Denmark, 2800 Kongens Lyngby, Denmark

³Deutsches Elektronen-Synchrotron DESY, Platanenallee 6, 15738 Zeuthen, Germany and Deutsches Zentrum für Astrophysik, Postplatz 1, 02826 Görlitz, Germany

^{a)} Author to whom correspondence should be addressed: dennis.wilken@aei.uni-hannover.de

ABSTRACT

Squeezed light plays a crucial role in state-of-the-art quantum metrology and quantum information experiments. There is significant interest in utilizing squeezed states at high MHz and GHz frequencies. However, past efforts to build suitable photodetectors at these frequencies have yet to yield the required high quantum efficiency. Here, we present the development of a high-frequency balanced photodetector with near-unity quantum efficiency, realized with off-the-shelf components. The detector operates in balanced mode up to approximately 500 MHz, above which the differential frequency response limits its performance. To obtain high sensitivity above 500 MHz, the detector can be efficiently used in an unbalanced homodyne detection scheme. We employ our detector in this unbalanced mode to measure a squeezing comb up to 6.4 GHz, achieving a squeezing level of up to 10.7 dB. By sharing our experience, specifically in identifying the unequal frequency response as a limiting factor, we aim to enable and advance further developments in the field.

© 2025 Author(s). All article content, except where otherwise noted, is licensed under a Creative Commons Attribution (CC BY) license (<https://creativecommons.org/licenses/by/4.0/>). <https://doi.org/10.1063/5.0290396>

Non-classical states—so-called squeezed states—are a valuable resource for quantum metrology and quantum information. They can help achieve higher sensitivity whenever experiments are limited by the quantum noise of the employed laser light. The most advanced application to date is the sensitivity enhancement of gravitational wave detectors.^{1–4} Other, lesser-known application examples include magnetometers,^{5–7} spectroscopy,^{8–11} or imaging.^{12–14} Beyond this, the entanglement inherent to squeezed states is highly interesting for experiments in quantum communication^{15,16} or computation.^{17–21} A single squeezing source can generate bipartite entanglement with THz bandwidth²² yielding an enormous scaling potential for multiplexing. Extending to cluster states,^{21,23–25} they enable large-scale measurement-based quantum computing.

So far, the highest levels of squeezing have been achieved when the required nonlinear process is enhanced in an optical resonator forming an optical parametric oscillator (OPO).²⁶ The resonance condition of the OPO leads to a comb structure in the squeezing spectrum, with the separation of the teeth corresponding to the free spectral range (FSR) of the resonator.^{27–30} However, in the future, waveguide

squeezers are aiming to achieve similar performance, providing a continuous squeezing spectrum.³¹ Their integration into a chip-based infrastructure paves the way for scalable quantum information platforms.^{32–35}

A key aspect of utilizing squeezed states is their detection. For phase-sensitive homodyne measurements, balanced photodetectors are preferred. These should possess near-unity quantum efficiency (quantum efficiency), a high shot noise to electronic dark noise clearance, sufficient bandwidth, and high common-mode rejection. Imperfect quantum efficiency acts as a loss channel, mixing the squeezed state with vacuum fluctuations and thereby degrading the observable squeezing level. High electronic detector noise obscures the squeezing signal and reduces the effective squeezing level, similar to losses. Squeezed light was primarily investigated at frequencies from the audio band to a few megahertz. Accordingly, detector development focused on these frequencies.^{36–40}

However, to fully exploit the bandwidth potential of squeezed light sources, detection at high frequencies is crucial. While significant efforts have been dedicated to developing balanced detectors with GHz

bandwidth,^{41–46} such devices have yet to reach high quantum efficiencies. Even measuring efficiently at the first FSR of an OPO with a large cavity length (corresponding to relatively low frequencies in the 500 MHz range) remains challenging.^{47–51} Consequently, alternative, but significantly more complex, approaches have been developed, which circumvent the need for simultaneous high quantum efficiency and high detection bandwidth. Bichromatic detection,^{52–55} for instance, uses a local oscillator with two frequencies to access the sidebands optically rather than electronically, and parametric amplification^{56–59} employs a second OPO to relax requirements on detector efficiency. Nevertheless, the gold standard for squeezed light detection remains broadband balanced homodyne detection with high quantum efficiency.

Here, we present the development of a high-frequency balanced photodetector with near-unity quantum efficiency at 1064 nm. The detector enables us to measure a quantum noise reduction at the first 31 FSRs of our squeezer, each separated by 200 MHz, corresponding to a spectrum spanning 6.2 GHz. At frequencies above approximately 500 MHz, we observe a reduction of the measured squeezing level, which we were able to trace to an imbalance in the complex frequency response of the two photodiodes in our circuit. To circumvent this limitation, we employ an unbalanced homodyne detection scheme, as already demonstrated in Ref. 30. In the current publication, we almost double the measurement range and show shot noise-limited performance up to 6.4 GHz.

Our detector's circuit diagram is shown in Fig. 1(a). Its simplicity is the result of a lengthy series of tests in which it was found that earlier, more complex variants did not provide any added value. The circuit can be divided into three parts: A detection stage, a DC stage, and an RF stage.

For the detection, we utilize two high-quantum efficiency photodiodes from Laser Components (IGHQEX0080) for operation at 1064 nm. These photodiodes have a specified quantum efficiency of $\geq 99\%$ and an active area with a diameter of $80\ \mu\text{m}$. We derived a lower bound for the quantum efficiency of $\geq 98.7\%$ from squeezing measurements.^{26,30} Across a batch of photodiodes, we could identify a few photodiodes with an approximately 0.2% increased quantum efficiency. The photodiode's capacitance is specified as 1 pF at a bias voltage of 2.5 V. We increased the bias voltage to 10 V to increase the

bandwidth and noise clearance. Our PCB is oriented horizontally, and we soldered the photodiodes to the side of the PCB and at right angles to each other, as shown in Fig. 1(b). We focus the light using 25 mm lenses mounted on fine adjustment stages (Newport LP-1B-XYZ). Apart from the photodiodes, the bypass capacitors (C_{1-4}) placed close to the photodiodes impact the high-frequency performance of the detector most significantly. At gigahertz frequencies, the impedance of these capacitors is dominated by the residual inductance of the package rather than the nominal capacitance value. Accordingly, we chose low inductance capacitors (Murata LLL185C70J105ME14) with a high capacitance of $1\ \mu\text{F}$.

The two photodiodes are installed back-to-back for direct current subtraction. A bias-T consisting of a capacitor (C_5) and an inductor (L_1) is used to separate the DC and RF signals. Changing their values allows a shift of the maximal clearance between dark noise and shot noise to higher frequencies. The values used here were chosen for best broadband performance. The DC is converted by a trans-impedance amplifier based on an Analog Devices AD797 operational amplifier. The DC signal is only used for alignment and control purposes and was not optimized for low-frequency squeezed light detection. The RF signal is amplified by a Mini-Circuits Mar-6 amplifier. It is powered via a current injection at its output using a second bias-T. The amplifier was chosen for its low noise figure and high gain. It has a nominal bandwidth of 2 GHz; similar amplifiers with higher bandwidth, such as the 7 GHz Mini-Circuits GALI-39+, showed a comparable behavior, indicating that the bandwidth of the detector is limited by the photodiodes and not the amplifier. We are only operating with a single RF amplifier stage for best noise performance, which was sufficient to separate the signal from our spectrum analyzer's (Keysight N9010b) noise floor, utilizing its pre-amplifier stage. Depending on the application, additional serial amplifiers can be added.

Our photodetector is based on off-the-shelf components and does not require sophisticated techniques to be built. We etched our PCBs in-house on conventional two-layer FR4 material but with a reduced thickness of 0.5 mm. Parts and vias were soldered by hand. For $50\ \Omega$ matching, components in the RF path were connected using microstrips. Tests with RF-optimized ceramic PCBs (Rogers RO4350) and automated assembly did not show any advantage. We designed an

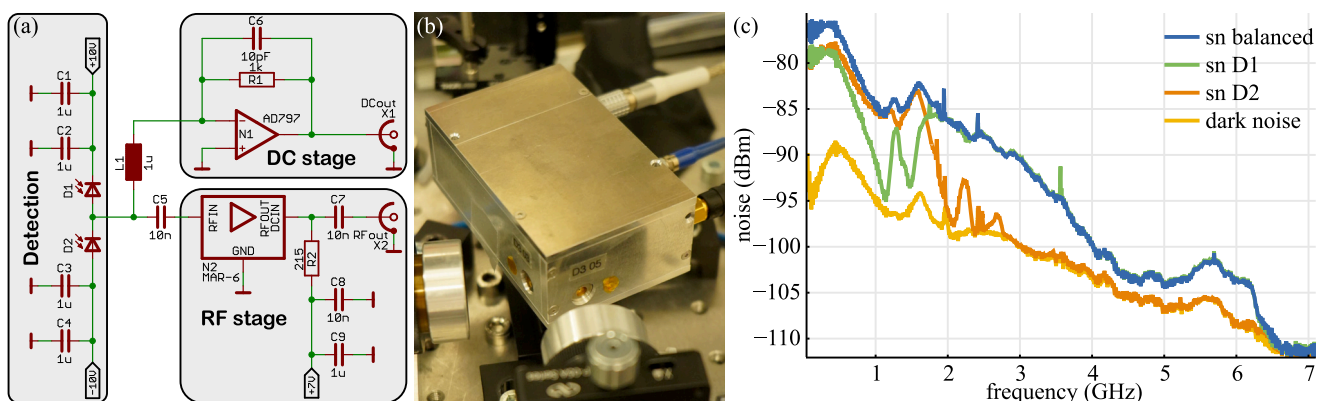


FIG. 1. (a) Schematic of the balanced photodetector. (b) Picture of the detector. (c) Measurement of the shot noise and dark noise levels of the detector with 8 mW per photodiode. The contributions of the two photodiodes D1 (green) and D2 (orange) to the combined shot noise level (blue) differ significantly.

aluminum housing for the detector shown in Fig. 1(b). A proper enclosure, as well as a good ground connection, were a crucial factor in mitigating the coupling of stray signals.

We measured the shot noise level of our detector with a power of 8 mW on each photodiode, as shown in Fig. 1(c). Below 300 MHz, the clearance between shot noise and detector dark noise reaches more than 15 dB at an incident power of 8 mW per photodiode. However, above approximately 500 MHz the shot noise levels of the two photodiodes, and therefore the frequency response, start deviating from each other, limiting the detector's capability to operate in balanced mode.

We measured the squeezing spectra of our 200 MHz-bowtie OPO unbalanced on one of the photodiodes. More details on the squeezed light source, detection, and phase control can be found in Ref. 30. As in the previous publication, the homodyne detection used a 99:1 beam splitter, but now its output voltage is measured by a spectrum analyzer with 7 GHz bandwidth. The normalized and dark noise-subtracted results are depicted in Figs. 2(a) and 2(b) for the two photodiodes. We measured squeezing levels of 11.0 dB (10.7 dB) at 200 MHz for photodiode D1 (D2). The difference can be explained by a 0.6% reduction of quantum efficiency caused by a defect visible on the diode's surface that only occurred after long usage. Over the full detection band, the measured squeezing level is fairly constant, with deviations discussed further below.

When operated as a balanced homodyne detector with a 50:50 beam splitter, we measured a squeezing level of 11.5 dB at 200 MHz, 11.2 dB at 400 MHz, and 10.6 dB at 600 MHz after dark noise subtraction, as shown in Fig. 2(c). For higher frequencies, the squeezing level starts to deteriorate more strongly, which can be explained by an unequal frequency response.

To understand this behavior, we characterized the frequency response of the two photodiodes with a 10 GHz fiber-coupled amplitude modulator (Exail NIR-MX- LN-10) and a 3 GHz-network analyzer (Keysight E5061b). The results are shown in Fig. 3(a).

We used the measured frequency response to predict the squeezing results for the balanced measurement. Since the common magnitude or phase response of the two photodiodes does not affect the normalized squeezing measurement, we focused on the photodiode's differential (complex) frequency response δ . It allows us to calculate the normalized variance of the photocurrent i_- ,⁵⁰

$$\text{var}(i_-)_{\text{norm}} = \frac{|1 + \delta|^2 \text{var}(\hat{X}_\theta) + |1 - \delta|^2}{|1 + \delta|^2 + |1 - \delta|^2}, \quad (1)$$

where \hat{X}_θ is the quadrature operator of the squeezed state under an arbitrary readout angle θ . For $\delta = 1$, this corresponds to the desired quadrature measurement \hat{X}_θ , whereas for $\delta = -1$ a variance of 1 is measured, corresponding to the shot noise of the local oscillator. The

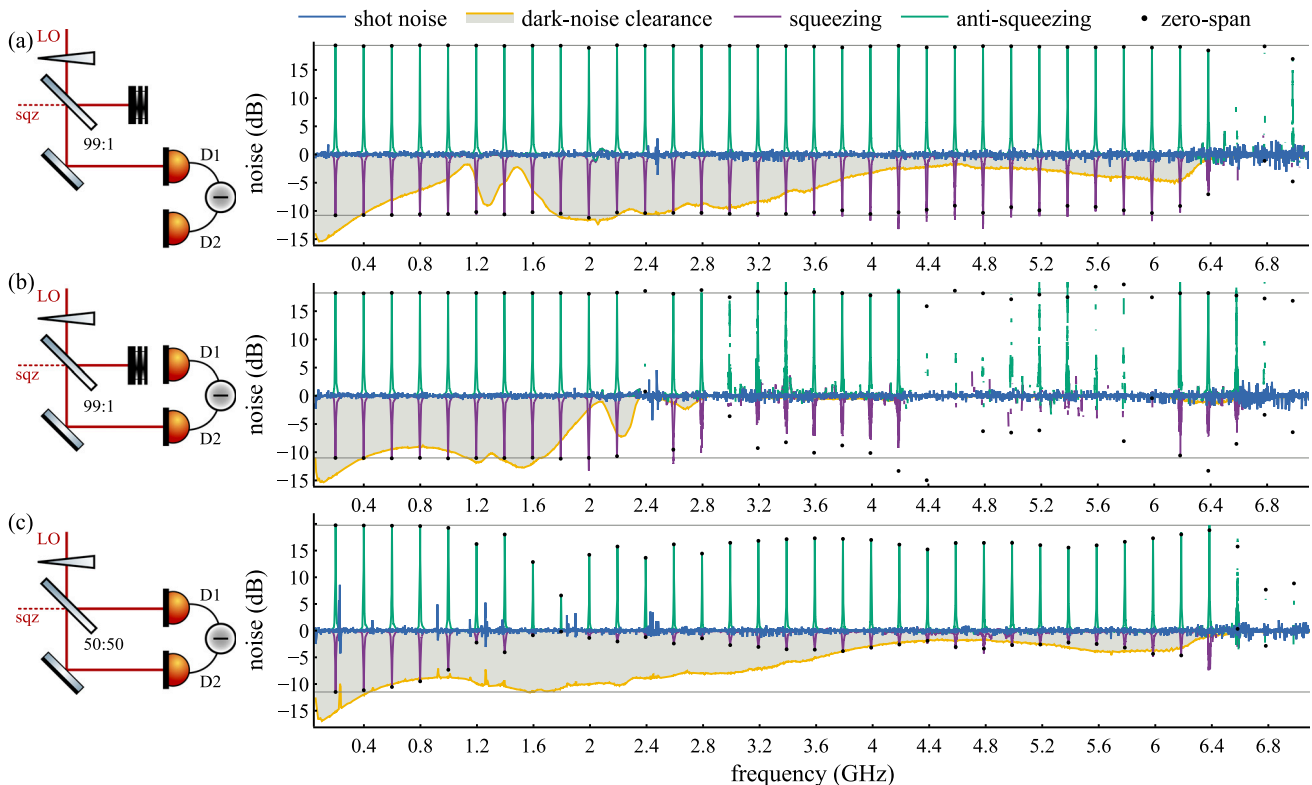


FIG. 2. Normalized squeezing comb measurements with unbalanced homodyne detection on photodiodes D1 (a) and D2 (b) and balanced homodyne detection (c). The electronic dark noise was subtracted from all traces and is indicated by the dark noise clearance. Accordingly, at higher frequencies, the squeezing levels are below the electronic noise. Additional zero-span measurements are used to determine the exact squeezing values at each FSR. The horizontal line indicates the squeezing level at the first FSR. A bowtie OPO with a round trip length of 1.5 m (corresponding to an FSR of 200 MHz) was used for the measurement.

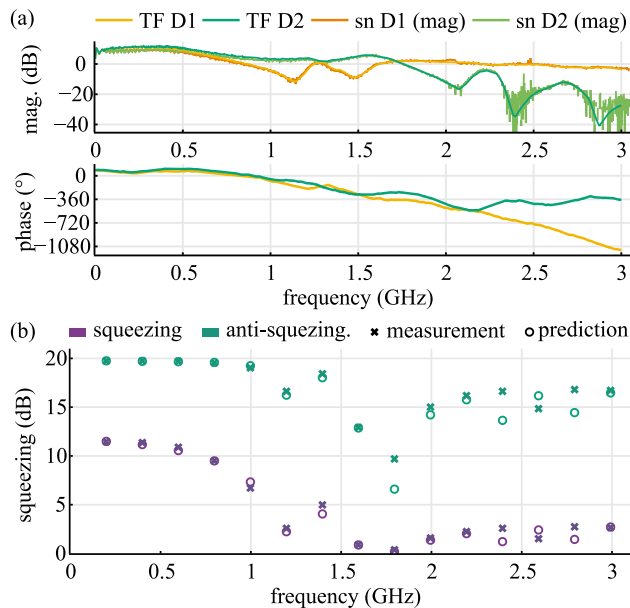


FIG. 3. (a) Transfer function measurement of the two photodiodes of the detector. Shot noise measurements (dark noise subtracted) are shown for reference, which follow the same magnitude response as the transfer function. (b) Comparison of measured and predicted squeezing levels for balanced detection. The behavior of the detector was modeled using the difference in frequency response of the two photodiodes. The bandwidth of the measurement of 3 GHz is given by the limited bandwidth of the network analyzer.

results are depicted in Fig. 3(b). The model is in high agreement with our experimental results within the measurement band, indicating that the photodiodes' asymmetric response is the limiting factor for the balanced operation of our detector.

Our detector is not affected by excess loss caused by distributed photocarrier generation, a process discussed in Ref. 48. Since shot noise is a white process, its measurement should equal the frequency response's magnitude. Deviations between the two measurements could indicate excess loss but could not be observed, as can be seen in Fig. 3(a). At frequencies above 3 GHz, we see a small drop in squeezing level of up to 1.6 dB for diode D1, which could indicate up to 3.8% excess loss at these frequencies. However, the work in Ref. 48 predicts a steady increase in loss over frequency, which we do not observe. Accordingly, we assume that the slight decrease in squeezing level might be a measurement artifact caused by the dominant electronic noise.

We performed linearity measurements of the detector. Figure 4(a) shows the detector's DC output voltage for each of the two photodiodes depending on the incident optical power. Up to 12 mW no indication of saturation can be seen. Figure 4(b) shows shot noise spectra for different powers. The dark noise was subtracted, and the traces were normalized to the 3.5 mW measurement to eliminate the common frequency response. Horizontal lines indicate the expected shot noise level. For D1, we only observe a drop in shot noise level at 10 mW at high frequencies. In contrast, D2 exhibits super-linear scaling for powers above 3.5 mW. While this could suggest nonlinear behavior of the detector, we conclude that the DC power only affects the photodiode's gain and that the detector's response to different noise levels remains

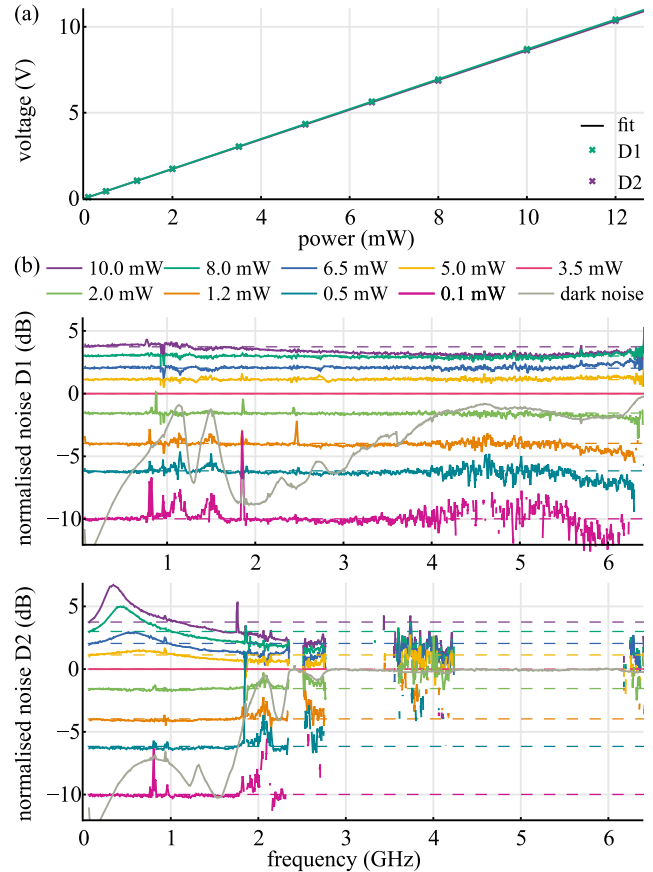


FIG. 4. (a) Photodetector's DC output voltage over incident optical power, including a linear fit. (b) Shot noise spectra for different power levels for diode D1 (top) and D2 (bottom). To flatten the measurements, all traces were normalized to the 3.5 mW measurement (pink). The detector's dark noise was subtracted from measurements and reference. The dashed horizontal lines indicate the expected shot noise level. Gaps in the traces are caused by subtracting the dark noise level when its value is greater than that of the measured shot noise.

linear. A good measure of linearity is provided by squeezing, anti-squeezing, and shot noise measurements that are performed at constant local oscillator power but probe different noise powers. For unbalanced operation, no irregularities were observed when comparing different frequencies or pump powers. For example, the unbalanced measurement on D2 shown in Fig. 2(b) was performed at 8 mW and shows constant noise levels over frequency below 1 GHz where the gain scales super-linearly. In contrast, the balanced measurement is much more affected. Here, we started to observe deviations between the measurements and our model [see Eq. (1) and Fig. 3(b)] for powers above 6 mW per diode.

In addition to Laser Component's high-quantum efficiency photodiodes, we also tested Fermionics' FD80W photodiodes, which are significantly cheaper yet still provide a high quantum efficiency of around 95%. Details can be found in Ref. 60. The photodiodes provided a much more symmetrical frequency response when installed in our detector. However, the measured squeezing levels deteriorate

much more severely, even under unbalanced detection, which limits the detector's bandwidth to a few hundred megahertz. This can be explained by a much more pronounced nonlinear behavior of the photodiodes.

We suspect that the packaging of the photodiodes leads to an asymmetric equivalent circuit. Consequently, the gain of the photodiodes depends on their installation orientation. The only way to address this issue is to modify the photodiode design. For instance, an SMD package could be used, or a second type of photodiode could be manufactured with an n-i-p junction instead of a p-i-n junction. Using an impedance matching network between the photodiodes and an amplifier could improve the photodiode gain, thereby improving the signal-to-noise ratio.

In conclusion, we present a high-frequency and high-quantum efficiency photodetector with a positive dark noise clearance up to 6.4 GHz, enabling homodyne measurements of strongly squeezed states at gigahertz frequencies. While this is a major achievement, our detector still shows limitations. Over large frequency ranges, the dark noise clearance, while positive, is rather low. We were able to identify the unequal frequency response of the two photodiodes as the limiting factor for balanced detection. This forces us to use an unbalanced detection scheme above approximately 500 MHz, which is effective but comes with limitations. Our work provides the first viable option for broadband, high-quantum efficiency homodyne detection. This is a crucial step in exploiting the scaling potential of squeezed states in quantum metrology and quantum information processing.

See the [supplementary material](#) for raw data and scripts for evaluating the data.

We would like to thank Elanor Huntington for the joint work on our first prototype detectors. Furthermore, we would like to thank Nived Johny, Bernd Schulte, and Manuel Schimanski for their support and for reviewing the manuscript. This work was funded by the Deutsche Forschungsgemeinschaft [Excellence PhoenixD (EXC 2122, Project ID 390833453) and the Excellence QuantumFrontiers (2EXC 2123, Project ID 390837967)].

AUTHOR DECLARATIONS

Conflict of Interest

The authors have no conflicts to disclose.

Author Contributions

Dennis Wilken: Conceptualization (lead); Formal analysis (lead); Investigation (lead); Methodology (lead); Visualization (lead); Writing—original draft (lead). **Jonas Junker:** Conceptualization (supporting); Formal analysis (supporting); Methodology (supporting); Resources (supporting); Writing/Review & Editing (equal). **Michèle Heurs:** Conceptualization (supporting); Funding acquisition (lead); Project administration (lead); Supervision (lead); Writing/Review & Editing (equal).

DATA AVAILABILITY

The data that support the findings of this study are available within the article and its [supplementary material](#).

REFERENCES

- ¹The LIGO Scientific Collaboration, "A gravitational wave observatory operating beyond the quantum shot-noise limit," *Nat. Phys.* **7**, 962 (2011).
- ²The Virgo Collaboration, "Increasing the astrophysical reach of the advanced virgo detector via the application of squeezed vacuum states of light," *Phys. Rev. Lett.* **123**, 231108 (2019).
- ³H. Yu, L. McCuller, M. Tse, N. Kijbunchoo, L. Barsotti, and N. Mavalvala, "Quantum correlations between light and the kilogram-mass mirrors of LIGO," *Nature* **583**, 43–47 (2020).
- ⁴W. Jia, V. Xu, K. Kuns, M. Nakano, L. Barsotti, M. Evans, N. Mavalvala, and Members of the LIGO Scientific Collaboration, "Squeezing the quantum noise of a gravitational-wave detector below the standard quantum limit," *Science* **385**, 1318–1321 (2024).
- ⁵F. Wolfgramm, A. Cerè, F. A. Beduini, A. Predojević, M. Koschorreck, and M. W. Mitchell, "Squeezed-light optical magnetometry," *Phys. Rev. Lett.* **105**, 053601 (2010).
- ⁶T. Horrom, R. Singh, J. P. Dowling, and E. E. Mikhailov, "Quantum-enhanced magnetometer with low-frequency squeezing," *Phys. Rev. A* **86**, 023803 (2012).
- ⁷C. Troullinou, R. Jiménez-Martínez, J. Kong, V. G. Lucivero, and M. W. Mitchell, "Squeezed-light enhancement and backaction evasion in a high sensitivity optically pumped magnetometer," *Phys. Rev. Lett.* **127**, 193601 (2021).
- ⁸Y. Michael, L. Bello, M. Rosenbluh, and A. Pe'er, "Squeezing-enhanced Raman spectroscopy," *npj Quantum Inf.* **5**, 1–9 (2019).
- ⁹M. Lassen, K. Berg-Sørensen, T. Gehring, R. B. de Andrade, H. Kerdoncuff, and U. L. Andersen, "Quantum-enhanced continuous-wave stimulated Raman scattering spectroscopy," *Optica* **7**(5), 470–475 (2020).
- ¹⁰J. Junker, D. Wilken, E. H. Huntington, and M. Heurs, "High-precision cavity spectroscopy using high-frequency squeezed light," *Opt. Express* **29**(4), 6053–6068 (2021).
- ¹¹F. Li, T. Li, M. O. Scully, and G. S. Agarwal, "Quantum advantage with seeded squeezed light for absorption measurement," *Phys. Rev. Appl.* **15**, 044030 (2021).
- ¹²A. Gatti, E. Brambilla, and L. Lugiato, "Quantum imaging," in *Progress in Optics*, edited by E. Wolf (Elsevier, 2008), Vol. 51, Chap. 5, pp. 251–348.
- ¹³M. A. Taylor, J. Janousek, V. Daria, J. Knittel, B. Hage, H.-A. Bachor, and W. P. Bowen, "Subdiffraction-limited quantum imaging within a living cell," *Phys. Rev. X* **4**, 011017 (2014).
- ¹⁴D. Soh and E. Chatterjee, "Label-free quantum super-resolution imaging using entangled multi-mode squeezed light," *New J. Phys.* **25**, 093001 (2023).
- ¹⁵M. Hillery, "Quantum cryptography with squeezed states," *Phys. Rev. A* **61**, 022309 (2000).
- ¹⁶*Quantum Information with Continuous Variables of Atoms and Light*, edited by N. J. Cerf, G. Leuchs, and E. S. Polzik (Imperial College Press, London, 2007).
- ¹⁷N. C. Menicucci, P. Van Loock, M. Gu, C. Weedbrook, T. C. Ralph, and M. A. Nielsen, "Universal quantum computation with continuous-variable cluster states," *Phys. Rev. Lett.* **97**, 110501 (2006).
- ¹⁸N. C. Menicucci, S. T. Flammia, and O. Pfister, "One-way quantum computing in the optical frequency comb," *Phys. Rev. Lett.* **101**, 130501 (2008).
- ¹⁹R. N. Alexander, P. Wang, N. Sridhar, M. Chen, O. Pfister, and N. C. Menicucci, "One-way quantum computing with arbitrarily large time-frequency continuous-variable cluster states from a single optical parametric oscillator," *Phys. Rev. A* **94**, 032327 (2016).
- ²⁰S. Takeda and A. Furusawa, "Toward large-scale fault-tolerant universal photonic quantum computing," *APL Photonics* **4**, 060902 (2019).
- ²¹B.-H. Wu, R. N. Alexander, S. Liu, and Z. Zhang, "Quantum computing with multidimensional continuous-variable cluster states in a scalable photonic platform," *Phys. Rev. Res.* **2**, 023138 (2020).
- ²²T. Kashiwazaki, T. Yamashita, N. Takahashi, A. Inoue, T. Umeki, and A. Furusawa, "Fabrication of low-loss quasi-single-mode PPLN waveguide and its application to a modularized broadband high-level squeezer," *Appl. Phys. Lett.* **119**, 251104 (2021).
- ²³M. Chen, N. C. Menicucci, and O. Pfister, "Experimental realization of multipartite entanglement of 60 modes of a quantum optical frequency comb," *Phys. Rev. Lett.* **112**, 120505 (2014).
- ²⁴X. Zhu, C.-H. Chang, C. González-Arciniegas, A. Pe'er, J. Higgins, and O. Pfister, "Hypercube cluster states in the phase-modulated quantum optical frequency comb," *Optica* **8**, 281–290 (2021).

- ²⁵M. V. Larsen, X. Guo, C. R. Breum, J. S. Neergaard-Nielsen, and U. L. Andersen, "Deterministic generation of a two-dimensional cluster state," *Science* **366**, 369–372 (2019).
- ²⁶H. Vahlbruch, M. Mehmet, K. Danzmann, and R. Schnabel, "Detection of 15 dB squeezed states of light and their application for the absolute calibration of photoelectric quantum efficiency," *Phys. Rev. Lett.* **117**, 110801 (2016).
- ²⁷A. E. Dunlop, E. H. Huntington, C. C. Harb, and T. C. Ralph, "Generation of a frequency comb of squeezing in an optical parametric oscillator," *Phys. Rev. A* **73**, 013817 (2006).
- ²⁸S. Shi, L. Tian, Y. Wang, Y. Zheng, C. Xie, and K. Peng, "Demonstration of channel multiplexing quantum communication exploiting entangled sideband modes," *Phys. Rev. Lett.* **125**, 070502 (2020).
- ²⁹S. Shi, Y. Wang, L. Tian, W. Li, Y. Wu, Q. Wang, Y. Zheng, and K. Peng, "Continuous variable quantum teleportation network," *Laser Photonics Rev.* **17**, 2200508 (2023).
- ³⁰D. Wilken, J. Junker, and M. Heurs, "Broadband detection of 18 teeth in an 11-dB squeezing comb," *Phys. Rev. Appl.* **21**, L031002 (2024).
- ³¹T. Kashiwazaki, T. Yamashima, K. Enbutsu, T. Kazama, A. Inoue, K. Fukui, M. Endo, T. Umeki, and A. Furusawa, "Over-8-dB squeezed light generation by a broadband waveguide optical parametric amplifier toward fault-tolerant ultra-fast quantum computers," *Appl. Phys. Lett.* **122**, 234003 (2023).
- ³²A. Dutt, K. Luke, S. Manapatruni, A. L. Gaeta, P. Nussenzeig, and M. Lipson, "On-chip optical squeezing," *Phys. Rev. Appl.* **3**, 044005 (2015).
- ³³Z. Yang, M. Jahanbozorgi, D. Jeong, S. Sun, O. Pfister, H. Lee, and X. Yi, "A squeezed quantum microcomb on a chip," *Nat. Commun.* **12**, 4781 (2021).
- ³⁴R. Gupta, R. Singh, A. Gehlot, S. V. Akram, N. Yadav, R. Brajpuriya, A. Yadav, Y. Wu, H. Zheng, A. Biswas, E. Suhir, V. S. Yadav, T. Kumar, and A. Singh Verma, "Silicon photonics interfaced with microelectronics for integrated photonic quantum technologies: A new era in advanced quantum computers and quantum communications?" *Nanoscale* **15**, 4682–4693 (2023).
- ³⁵K. Alexander, A. Benyamini, D. Black, D. Bonneau, S. Burgos, B. Burrige, H. Cable, G. Campbell, G. Catalano, A. Ceballos, C.-M. Chang, S. S. Choudhury, C. J. Chung, F. Danesh, T. Dauer, M. Davis, E. Dudley, P. Er-Xuan, J. Fargas, A. Farsi, C. Fenrich, J. Frazer, M. Fukami, Y. Ganesan, G. Gibson, M. Gimeno-Segovia, S. Goeldi, P. Goley, R. Haislmaier, S. Halimi, P. Hansen, S. Hardy, J. Horng, M. House, H. Hu, M. Jadidi, V. Jain, H. Johansson, T. Jones, V. Kamineni, N. Kelez, R. Koustubam, G. Kovall, P. Krogen, N. Kumar, Y. Liang, N. LiCausi, D. Llewellyn, K. Lokovic, M. Lovelady, V. R. Manfrinato, A. Melnichuk, G. Mendoza, B. Moores, S. Mukherjee, J. Munns, F.-X. Musalem, F. Najafi, J. L. O'Brien, J. E. Ortmann, S. Pai, B. Park, H.-T. Peng, N. Penthorn, B. Peterson, G. Peterson, M. Poush, G. J. Pryde, T. Ramprasad, G. Ray, A. V. Rodriguez, B. Roxworthy, T. Rudolph, D. J. Saunders, P. Shadbolt, D. Shah, A. Bahgat Shehata, H. Shin, J. Sinsky, J. Smith, B. Sohn, Y.-I. Sohn, G. Son, M. C. M. M. Souza, C. Sparrow, M. Staffaroni, C. Stavrakas, V. Sukumaran, D. Tamborini, M. G. Thompson, K. Tran, M. Triplett, M. Tung, A. Veitia, A. Vert, M. D. Vidrighin, I. Vorobeichik, P. Weigel, M. Wingert, J. Wooding, X. Zhou, and PsiQuantum Team, "A manufacturable platform for photonic quantum computing," *Nature* **641**, 876–883 (2025).
- ³⁶M. S. Stefszky, C. M. Mow-Lowry, S. S. Y. Chua, D. A. Shaddock, B. C. Buchler, H. Vahlbruch, A. Khalaidovski, R. Schnabel, P. K. Lam, and D. E. McClelland, "Balanced homodyne detection of optical quantum states at audio-band frequencies and below," *Classical Quantum Gravity* **29**, 145015 (2012).
- ³⁷X. Jin, J. Su, Y. Zheng, C. Chen, W. Wang, and K. Peng, "Balanced homodyne detection with high common mode rejection ratio based on parameter compensation of two arbitrary photodiodes," *Opt. Express* **23**, 23859–23866 (2015).
- ³⁸J.-R. Wang, Q.-W. Wang, L. Tian, J. Su, and Y.-H. Zheng, "A low-noise, high-SNR balanced homodyne detector for the bright squeezed state measurement in 1–100 kHz range," *Chin. Phys. B* **29**, 034205 (2020).
- ³⁹J. Wang, S. Wu, L. Hou, C. Mi, X. Shi, and X. Gao, "A low-noise, high-SNR and large-dynamic-range balanced homodyne detector for broadband squeezed light measurement," *Results Phys.* **57**, 107356 (2024).
- ⁴⁰L. Gao, L.-a Zheng, B. Lu, S. Shi, L. Tian, and Y. Zheng, "Generation of squeezed vacuum state in the millihertz frequency band," *Light* **13**, 294 (2024).
- ⁴¹X. Zhang, Y. Zhang, Z. Li, S. Yu, and H. Guo, "1.2-GHz balanced homodyne detector for continuous-variable quantum information technology," *IEEE Photonics J.* **10**, 6803810 (2018).
- ⁴²D. Milovancev, F. Honz, N. Vokic, M. Achleitner, F. Laudenbach, C. Pacher, H. Hubel, and B. Schrenk, "Chip-level GHz capable balanced quantum homodyne receivers," *J. Lightwave Technol.* **40**, 7518–7528 (2022).
- ⁴³J. F. Tasker, J. Frazer, G. Ferranti, E. J. Allen, L. F. Brunel, S. Tanzilli, V. D'Auria, and J. C. Matthews, "Silicon photonics interfaced with integrated electronics for 9 GHz measurement of squeezed light," *Nat. Photonics* **15**, 11–15 (2021).
- ⁴⁴B. Bai, J. Huang, G. R. Qiao, Y. Q. Nie, W. Tang, T. Chu, J. Zhang, and J. W. Pan, "18.8 Gbps real-time quantum random number generator with a photonic integrated chip," *Appl. Phys. Lett.* **118**, 264001 (2021).
- ⁴⁵C. Bruynsteen, M. Vanhocke, J. Bauwelinck, and X. Yin, "Integrated balanced homodyne photonic-electronic detector for beyond 20 GHz shot-noise-limited measurements," *Optica* **8**, 1146 (2021).
- ⁴⁶G. N. Milford, C. C. Harb, and E. H. Huntington, "Shot noise limited, microwave bandwidth photodetector design," *Rev. Sci. Instrum.* **77**, 114701 (2006).
- ⁴⁷T. Serikawa and A. Furusawa, "500 MHz resonant photodetector for high-quantum-efficiency, low-noise homodyne measurement," *Rev. Sci. Instrum.* **89**, 063120 (2018).
- ⁴⁸T. Serikawa and A. Furusawa, "Excess loss in homodyne detection originating from distributed photocarrier generation in photodiodes," *Phys. Rev. Appl.* **10**, 064016 (2018).
- ⁴⁹D. W. Gould, V. B. Adya, S. S. Y. Chua, J. Junker, D. Wilken, T. G. McRae, B. J. J. Slagmolen, M. J. Yap, R. L. Ward, M. Heurs, and D. E. McClelland, "Quantum enhanced balanced heterodyne readout for differential interferometry," *Phys. Rev. Lett.* **133**, 063602 (2024).
- ⁵⁰B. Tohermes, S. Verclas, and R. Schnabel, "Directly measured squeeze factors over GHz bandwidth from monolithic ppKTP resonators," [arXiv:2412.03221](https://arxiv.org/abs/2412.03221) (2024).
- ⁵¹J. Junker, J. Qin, V. B. Adya, N. Kijbunchoo, S. S. Y. Chua, T. G. McRae, B. J. J. Slagmolen, and D. E. McClelland, "Squeezing at the normal-mode splitting frequency of a nonlinear coupled cavity," *Phys. Rev. Lett.* **134**, 243603 (2025).
- ⁵²A. M. Marino, C. R. Stroud, Jr., V. Wong, R. S. Bennink, and R. W. Boyd, "Bichromatic local oscillator for detection of two-mode squeezed states of light," *J. Opt. Soc. Am. B* **24**(2), 335–339 (2007).
- ⁵³S. Shi, J. Wang, L. Tian, X. Sun, Y. Wang, and Y. Zheng, "Observation of a comb of squeezed states with a strong squeezing factor by a bichromatic local oscillator," *Opt. Lett.* **45**(8), 2419–2422 (2020).
- ⁵⁴C. S. Embrey, J. Hordell, V. Boyer, and P. G. Petrov, "Bichromatic homodyne detection of broadband quadrature squeezing," *Opt. Express* **24**(24), 27298–27308 (2016).
- ⁵⁵B. Xie, S. Feng, and D. He, "Quantum theory of phase-sensitive heterodyne detection," *J. Opt. Soc. Am. B* **33**(7), 1365–1372 (2016).
- ⁵⁶Y. Shaked, Y. Michael, R. Z. Vered, L. Bello, M. Rosenbluh, and A. Pe'er, "Lifting the bandwidth limit of optical homodyne measurement with broadband parametric amplification," *Nat. Commun.* **9**, 1–12 (2018).
- ⁵⁷N. Takanashi, R. Kasahara, K. Enbutsu, T. Umeki, A. Furusawa, T. Kashiwazaki, T. Kazama, and A. Inoue, "All-optical phase-sensitive detection for ultra-fast quantum computation," *Opt. Express* **28**(23), 34916–34926 (2020).
- ⁵⁸Y. Tian, X. Sun, Y. Wang, Y. Wang, Y. Wang, Q. Li, L. Tian, L. Tian, Y. Zheng, Y. Zheng, and Y. Zheng, "Cavity enhanced parametric homodyne detection of a squeezed quantum comb," *Opt. Lett.* **47**(3), 533–536 (2022).
- ⁵⁹A. Inoue, T. Kashiwazaki, T. Yamashima, N. Takanashi, T. Kazama, K. Enbutsu, K. Watanabe, T. Umeki, M. Endo, and A. Furusawa, "Toward a multi-core ultra-fast optical quantum processor: 43-GHz bandwidth real-time amplitude measurement of 5-dB squeezed light using modularized optical parametric amplifier with 5G technology," *Appl. Phys. Lett.* **122**, 104001 (2023).
- ⁶⁰D. M. Wilken, "A high-frequency squeezing comb - generation, detection & characterisation," *Ph.D. thesis* (Institutionelles Repositorium der Leibniz Universität Hannover, Hannover, 2024).